Journal of Hydroscience and Hydraulic Engineering
Vol. 23, No.1 May, 2005, 43-55

PARAMETERIZATION FOR CO_2 TRANSFER VELOCITY AT THE SURFACE OF WIND WAVES

By

Hiromichi TSUMORI, Yuji SUGIHARA

Dept. of Earth System Science and Technology, Kyushu University,
6-1 Kasuga-koen, Kasuga 816-8580, Japan

and

Akira MASUDA

Research Institute for Applied Mechanics, Kyushu University,
6-1 Kasuga-koen, Kasuga 816-8580, Japan

SYNOPSIS

Laboratory experiments were made to parameterize accurately the gas transfer velocity of carbon dioxide (CO_2) at the surface of wind waves. The local flux of CO_2 was estimated at several fetches in a wind-wave tank by fitting logarithmic laws to vertical profiles of the mean wind speed and the mean concentration of CO_2 in the air. The concentration of CO_2 dissolved in the water was quantified by means of a gas-liquid equilibrator made of a hydrophobic porous tube. The local gas transfer velocity at the water surface was obtained from the local flux and the difference between the bulk concentration in the water and the equilibrium concentration at the water surface. The transfer velocity increases steadily with the friction velocity, and also increases with the fetch under the condition of the same friction velocity. For the parameterization, two dimensionless parameters gx/u_{*a}^2 and $u_{*a}^3/g\nu_a$, were derived from a dimensional analysis, where u_{*a} is the friction velocity on the air side, g the acceleration of gravity, x the fetch and ν_a the kinematic viscosity of the air. On the basis of the experimental results and the dimensional analysis, we proposed a new type of empirical expression for the transfer velocity in consideration of the fetch dependence. With the fetch relations for wind waves, the expression can be described in terms of local dimensionless wind-wave parameters, i.e., $gE^{1/2}/u_{*a}^2$ or $\omega_p u_{*a}/g$ instead of gx/u_{*a}^2, where E represents the total energy of the surface displacement and ω_p the spectral peak angular frequency of wind waves.

INTRODUCTION

In order to predict the variations of atmospheric and oceanic environments, it is necessary to estimate the gas transfer velocity across the air-sea interface. Most empirical expressions for the transfer velocity have been formulated as a function of the mean wind speed referred to 10 m height. Such expressions are certainly practical in the sense that the transfer velocity can be estimated from information about the wind speed. However, the developments of wind waves and turbulent boundary layer depend strongly on the fetch of the sea surface. Therefore, characteristic quantities concerning the fetch, such as the wave height and the peak frequency of wind waves, should be added to variables in the parameterization for the transfer velocity.

Zhao et al. (1) attempted to parameterize the gas transfer velocity of CO_2 at the surface of wind waves on the basis of experimental data of Jähne et al. (2). By introducing a dimensionless parameter R_B proposed by Toba and Koga (3), they formulated the following expression for the transfer velocity k_L (cm/h):

$$k_L = 0.25 R_B^{0.67} \tag{1}$$

where R_B is defined as $u_{*a}^2/\nu_a\omega_p$, with ν_a being the kinematic viscosity of the air and ω_p the spectral peak angular frequency of wind waves. R_B seems to be closely connected with hydrodynamic properties of turbulent boundary layer close to the air-sea interface. However, this expression cannot be universally described because the dimensional quantity k_L is combined with the dimensionless parameter.

The transfer velocity for various gases has frequently been investigated through laboratory wind-wave experiments. However, in earlier experiments, only the overall gas transfer velocity averaged over the whole interface in a wind-wave tank was measured. The dependence of the transfer velocity on the fetch has not been examined sufficiently despite the fact that the friction velocity and wave characteristics vary obviously with the fetch. A few laboratory studies have been carried out concerning the fetch dependence of the CO_2 transfer velocity. A laboratory study conducted by Komori et al. (4) is a typical one in which the transfer velocity has been locally measured. A control volume was set over the region of the fetch = 3 to 5 m on the air side in a wind-wave tank, and they obtained the local CO_2 flux across the air-water interface from the budget of CO_2 within the volume. As an alternative method of quantifying the local flux at a certain fetch, we may think of the eddy correlation method and the profile method. However, the former is not suitable for laboratory experiments since an ultrasonic velocimeter is required to measure the wind speed fluctuations, and furthermore, it is too large to use in a wind-wave tank. On the other hand, the latter method, by which we can obtain the local flux from vertical profiles of the wind speed and the concentration of CO_2 in the air, seems to be appropriate for laboratory experiments.

The purpose of this study is to parameterize accurately the gas transfer velocity of CO_2 at the surface of wind waves. Vertical profiles of the mean wind speed and the mean concentration of CO_2 in the air were measured in a wind-wave tank, and the local CO_2 flux was estimated at several fetches by the profile method. The concentration of CO_2 dissolved in the water was quantified by means of a gas-liquid equilibrator made of a hydrophobic porous tube. The local transfer velocity on the water side was determined from these experimental results. Finally, on the basis of the experimental results and a dimensional analysis, we proposed new empirical expressions for the transfer velocity in view of the fetch dependence.

ESTIMATION OF GAS TRANSFER VELOCITY

In order to evaluate the local CO_2 flux at a certain fetch F (mol/m^{2}s), the profile method was used. For the turbulent transfer of passive scalar, the turbulent Schmidt number ν_t/K_t, where ν_t (m^2/s) is the eddy viscosity and K_t (m^2/s) the eddy diffusivity of CO_2, is close to the unity. By means of the mixing-length model, we obtain

$$F = -K_t\frac{\partial C_a}{\partial z} \approx -\nu_t\frac{\partial C_a}{\partial z} = -\kappa u_{*a} z\frac{\partial C_a}{\partial z} \tag{2}$$

where C_a (mol/m^3) is the mean concentration of CO_2 in the air, z the vertical coordinate axis taken upward from the still water surface, u_{*a} (m/s) the friction velocity on the air side and κ the von Kármán constant (= 0.4). After performing the integration for both sides of Eq. 2, we obtain

$$C_a(z_0) - C_a(z) = \frac{F}{\kappa u_{*a}} \ln\left(\frac{z}{z_0}\right) \tag{3}$$

where $C_a(z_0)$ denotes the concentration at the height of the roughness length z_0. Let us consider

$$F = C_* u_{*a} \tag{4}$$

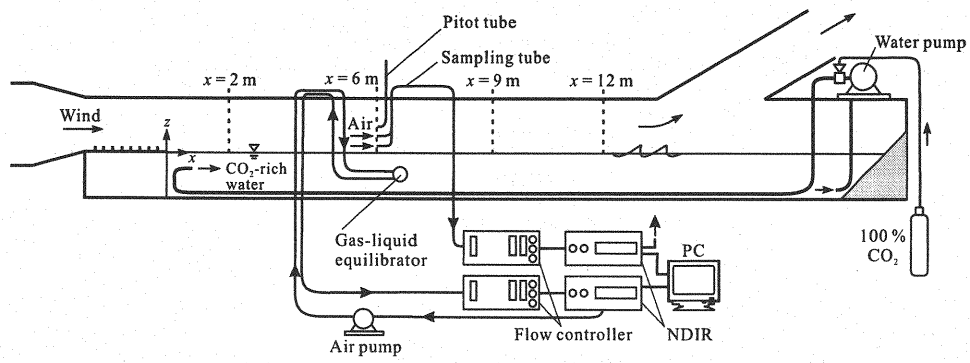

Fig. 1 Schematic diagram of experimental apparatus.

to define a representative concentration C_* (mol/m^3). Substitution of Eq. 4 to Eq. 3 gives a logarithmic law for the mean concentration in the air:

$$\frac{C_a(z_0) - C_a(z)}{C_*} = \frac{1}{\kappa} \ln\left(\frac{z}{z_0}\right) \tag{5}$$

In this way, we can obtain the local flux at a certain fetch from the product of C_* and u_{*a}, which are evaluated by fitting each logarithmic law to experimental data. Consequently, the local gas transfer velocity on the water side k_L (m/s) can be estimated from the following relation:

$$F = C_* u_{*a} = k_L(C_w - C_s) \tag{6}$$

where C_w (mol/m^3) is the concentration of CO_2 in the bulk of water, and C_s (mol/m^3) the equilibrium concentration on the the water side balanced with the concentration on the air side at the air-water interface.

EXPERIMENTAL PROCEDURE

Experiments were carried out using a wind-wave tank as illustrated schematically in Fig. 1. The tank was 17 m long, 0.60 m wide and 0.80 m deep, and the water depth was kept at 0.39 m. The horizontal coordinate axis x was taken leeward from the upwind edge in the tank, i.e., x denotes the fetch. In order to measure the CO_2 flux from the water side to the air side, the concentration of CO_2 in the water was increased in advance to about 40,000 ppm by injecting the 100% CO_2 into the water in the tank. After aeration, wind waves were generated by blowing the air above the water surface. Vertical profiles of the wind speed and the concentration of CO_2 in the air, and wind-wave characteristics were measured at a fetch of 2.0, 6.0, 9.0 and 12.0 m along the centerline of the tank. In the experiments, wind wave fields were in the statistical stationary state, therefore, the duration was not taken into account.

Experimental parameters are summarized in Table 1. The reference wind speed at the entrance of the wind tunnel Ur varied from 4.0 to 12.0 m/s. The vertical profile of the mean wind speed was measured by means of a Pitot tube in the range of 0.30 m above the still water surface. The friction velocity on the air side u_{*a} and the roughness length z_0 were calculated by fitting the logarithmic law to the vertical profile of the mean wind speed. The displacement of the water surface was measured by using capacitance wave gauges. The significant wave height H_s, the total energy of the displacement E and the spectral peak angular frequency of wind waves ω_p were evaluated from the measurements. The values of u_{*a}, z_0, H_s, E and ω_p are also listed in Table 1.

Fig. 2(a) shows a schematic diagram of the measuring system of the concentration of CO_2 in the air. The air in the wind tunnel was sampled by two inlet tubes in the range of $z \leqq 0.20$ m, and the sampling flow rate was about 1 l/min. The control of the sampling rate and the dehumidification of the air were made by a flow controller

Table 1 Experimental parameters.

Fetch [m]	Ur [m/s]	u_{*a} [m/s]	z_0 [m]	H_s [m]	E [m^2]	ω_p [1/s]	ΔpCO_2 [μatm]	k_L [m/s]
	4.0	0.169	4.34×10^{-5}	4.46×10^{-4}	1.47×10^{-8}	55.1	3.03×10^{4}	4.89×10^{-5}
	5.0	0.224	2.73×10^{-5}	1.36×10^{-3}	1.38×10^{-7}	51.4	3.15×10^{4}	6.30×10^{-5}
	6.0	0.253	2.89×10^{-5}	2.27×10^{-3}	3.75×10^{-7}	48.2	3.83×10^{4}	8.67×10^{-5}
	7.0	0.305	2.54×10^{-5}	3.49×10^{-3}	8.99×10^{-7}	41.9	2.94×10^{4}	1.03×10^{-4}
2.0	8.0	0.351	3.18×10^{-5}	6.02×10^{-3}	2.69×10^{-6}	32.8	3.70×10^{4}	1.22×10^{-4}
	9.0	0.413	4.37×10^{-5}	7.87×10^{-3}	4.71×10^{-6}	33.1	3.25×10^{4}	1.27×10^{-4}
	10.0	0.456	3.82×10^{-5}	9.79×10^{-3}	7.45×10^{-6}	29.1	2.99×10^{4}	1.32×10^{-4}
	11.0	0.519	4.59×10^{-5}	1.14×10^{-2}	9.85×10^{-6}	27.8	3.13×10^{4}	1.40×10^{-4}
	12.0	0.571	4.75×10^{-5}	1.30×10^{-2}	1.32×10^{-5}	26.8	2.62×10^{4}	1.50×10^{-4}
	4.0	0.225	1.75×10^{-4}	3.12×10^{-3}	6.61×10^{-7}	40.3	4.06×10^{4}	9.61×10^{-5}
	5.0	0.279	1.31×10^{-4}	6.59×10^{-3}	2.97×10^{-6}	31.3	3.69×10^{4}	1.37×10^{-4}
	6.0	0.343	1.80×10^{-4}	1.01×10^{-2}	6.91×10^{-6}	25.9	3.45×10^{4}	1.62×10^{-4}
	7.0	0.410	1.97×10^{-4}	1.59×10^{-2}	1.79×10^{-5}	22.1	3.79×10^{4}	1.70×10^{-4}
6.0	8.0	0.464	1.70×10^{-4}	1.87×10^{-2}	2.37×10^{-5}	20.6	3.60×10^{4}	1.93×10^{-4}
	9.0	0.524	1.60×10^{-4}	2.16×10^{-2}	3.26×10^{-5}	18.7	3.66×10^{4}	2.13×10^{-4}
	10.0	0.598	1.81×10^{-4}	2.38×10^{-2}	3.89×10^{-5}	18.4	3.18×10^{4}	2.33×10^{-4}
	11.0	0.712	2.63×10^{-4}	2.86×10^{-2}	5.71×10^{-5}	16.6	2.84×10^{4}	2.74×10^{-4}
	12.0	0.844	4.43×10^{-4}	3.27×10^{-2}	7.13×10^{-5}	16.1	2.79×10^{4}	3.42×10^{-4}
	4.0	0.237	1.53×10^{-4}	6.15×10^{-3}	2.53×10^{-6}	31.3	3.12×10^{4}	1.17×10^{-4}
	5.0	0.287	1.34×10^{-4}	1.07×10^{-2}	7.88×10^{-6}	24.5	3.28×10^{4}	1.43×10^{-4}
	6.0	0.339	1.40×10^{-4}	1.63×10^{-2}	1.85×10^{-5}	21.5	3.74×10^{4}	1.68×10^{-4}
	7.0	0.439	1.78×10^{-4}	2.16×10^{-2}	3.21×10^{-5}	18.3	3.69×10^{4}	2.18×10^{-4}
9.0	8.0	0.495	1.75×10^{-4}	2.63×10^{-2}	4.67×10^{-5}	16.9	3.07×10^{4}	2.51×10^{-4}
	9.0	0.595	2.52×10^{-4}	3.13×10^{-2}	6.66×10^{-5}	16.0	3.27×10^{4}	2.87×10^{-4}
	10.0	0.726	3.89×10^{-4}	3.42×10^{-2}	7.81×10^{-5}	14.7	3.12×10^{4}	3.35×10^{-4}
	11.0	0.811	4.84×10^{-4}	4.08×10^{-2}	1.12×10^{-4}	14.4	3.14×10^{4}	4.06×10^{-4}
	12.0	0.990	9.49×10^{-4}	5.13×10^{-2}	1.81×10^{-4}	13.0	3.28×10^{4}	4.96×10^{-4}
	4.0	0.235	1.97×10^{-4}	8.90×10^{-3}	5.41×10^{-6}	24.2	3.47×10^{4}	1.25×10^{-4}
	5.0	0.284	1.73×10^{-4}	1.57×10^{-2}	1.67×10^{-5}	21.3	3.25×10^{4}	1.85×10^{-4}
	6.0	0.344	1.30×10^{-4}	2.04×10^{-2}	2.77×10^{-5}	18.1	3.71×10^{4}	2.24×10^{-4}
	7.0	0.451	2.16×10^{-4}	2.77×10^{-2}	5.44×10^{-5}	16.1	3.67×10^{4}	2.80×10^{-4}
12.0	8.0	0.545	2.71×10^{-4}	3.11×10^{-2}	6.36×10^{-5}	15.2	2.90×10^{4}	3.26×10^{-4}
	9.0	0.666	3.92×10^{-4}	3.79×10^{-2}	9.99×10^{-5}	14.1	4.09×10^{4}	3.91×10^{-4}
	10.0	0.771	4.76×10^{-4}	4.44×10^{-2}	1.31×10^{-4}	13.0	3.30×10^{4}	4.87×10^{-4}
	11.0	0.951	9.12×10^{-4}	5.73×10^{-2}	2.16×10^{-4}	12.6	2.77×10^{4}	6.10×10^{-4}
	12.0	1.17	1.64×10^{-3}	6.24×10^{-2}	2.54×10^{-4}	11.4	2.54×10^{4}	7.41×10^{-4}

instrument. The concentration in the air was measured by means of a non-dispersive infrared gas analyzer (NDIR, LI-COR LI-6252). The NDIR was calibrated with 198 and 498 ppm standard CO_2 gases. The data were recorded on a personal computer at a sampling rate of 1 Hz. Though the air was sampled for 90 s at each level, only the data for the latter 60 s were used for evaluating the mean concentration in consideration of the exchange of the air in the sampling tubes.

The measuring system of the dissolved concentration of CO_2 in the water is schematically shown in Fig. 2(b). The partial pressure of CO_2 in the water was evaluated by using a gas-liquid equilibrator made of hydrophobic porous tube. A large number of small holes exist on the surface of the tube, and the diameter of the holes was about 1 μm. The CO_2 gas can be exchanged between the equilibrator and the water through such holes. An air-circulating circuit through the gas-liquid equilibrator and NDIR was made as shown in the figure. The air CO_2 flowing in the hydrophobic porous tube rapidly equilibrated with the dissolved CO_2. The equilibrated gas was dehumidified by both the Peltier dryer and the magnesium perchlorate ($Mg(ClO_4)_2$). The partial pressure of the equilibrated gas pCO_2 (μatm) was evaluated by a NDIR (RMT DX-6100), which was able to measure up to

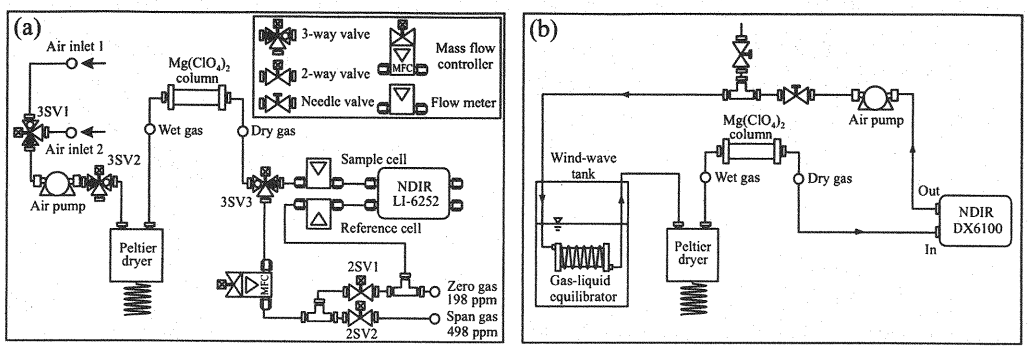

Fig. 2 Measuring system of the concentration of CO_2. (a) on the air side and (b) on the water side.

50,000 ppm. We estimated the concentration of CO_2 in the water C_w by using the following relation:

$$C_w = S \cdot pCO_2 \tag{7}$$

where S (mol/m^3 $\cdot$ μatm) is the solubility of CO_2 on the water side calculated by a function of Weiss (5). The position of the gas-liquid equilibrator was changed depending on experimental conditions. The equilibrator was located at 0.20 m below the water surface and 0.50 m backward from the measuring position on the air side.

The mean concentration in the water during the flux measurement was used as C_w in Eq. 6 because the concentration decreases temporally. The partial pressure on the air side at the interface PCO_{2s} (μatm) was obtained by extrapolating the concentration profile to $z = 0$, and C_s was calculated from

$$C_s = S \cdot PCO_{2s} \tag{8}$$

The difference between the partial pressures ΔpCO_2 (= $pCO_2 - PCO_{2s}$) and the gas transfer velocity k_L are given in Table 1. It should be noted that the values of k_L in the table were converted to those for the fresh water at the standard reference temperature 20°C, i.e., for the Schmidt number Sc = 600, by means of the Schmidt number dependence suggested by Jähne et al. (6):

$$k_{L\,600} = \left(\frac{600}{Sc(T)}\right)^{-\frac{1}{2}} k_L(T) \tag{9}$$

where $Sc(T)$ and $k_L(T)$ denote the Schmidt number and the transfer velocity at the temperature of T°C, respectively. Here, Sc is defined as ν_w/D, where ν_w is the kinematic viscosity of the water and D the molecular diffusivity of CO_2 in the water. The values of $Sc(T)$ were computed by a function of Wanninkhof (7).

RESULTS AND DISCUSSION

Fig. 3 shows the vertical profiles of the mean concentration of CO_2 in the air at each fetch in the case of Ur = 6.0 m/s, where the solid lines denote the fitting curves for the logarithmic law obtained by the least square method. Although the concentration of dissolved CO_2 is unequal for each case, it can be observed that the vertical gradient of the concentration increases with the fetch. It is also evident that logarithmic layers are formed close to the water surface. The values of C_* were calculated by applying Eq. 5 to these logarithmic layers.

The profiles of the concentration in the air are normalized by using z_0 and u_{*a}, and are compared with Eq. 5 in Fig. 4, where the solid line indicates Eq. 5 and all the data are plotted. There is a large scattering of the data around the solid line in the region of $z/z_0 > 3.0 \times 10^2$ since the logarithmic law is applicable only to the profile at small z; the applicable range varies depending on both the wind speed and the fetch. It is observed from the figure that the data agree accurately with Eq. 5 in the vicinity of the water surface. This means that C_* estimated from the experimental results is reasonably accurate.

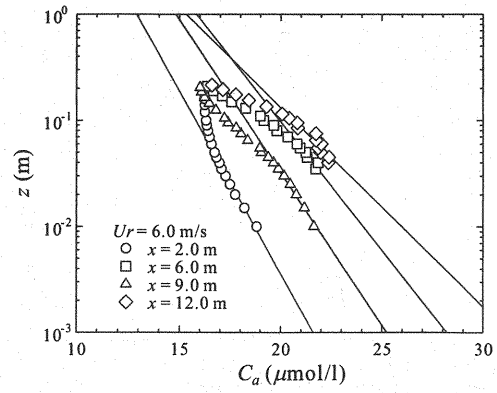

Fig. 3 Vertical profiles of the mean concentration of CO_2 in the air.

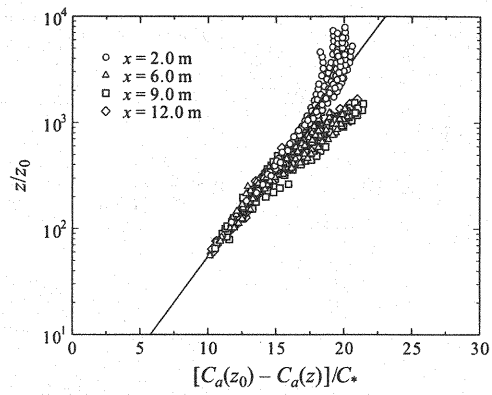

Fig. 4 Normalized vertical profiles of the mean concentration of CO_2 in the air.

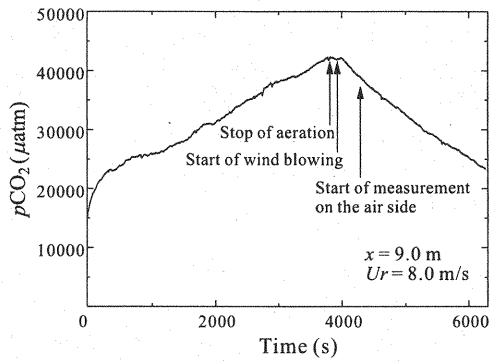

Fig. 5 Time variation of pCO_2.

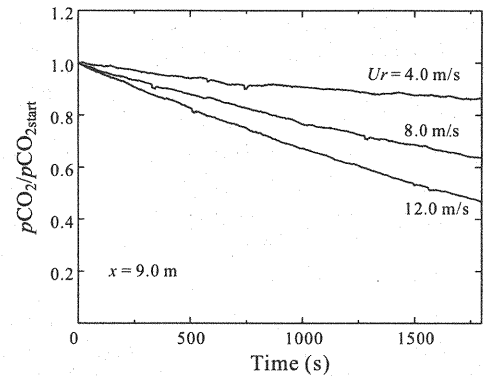

Fig. 6 Dependence of reduction rate of pCO_2 on the wind speed.

Fig. 5 shows the time variation of the partial pressure in the water pCO_2, from the start of the aeration to the end of the measurement under the condition of x = 9.0 m and Ur = 8.0 m/s. The partial pressure increases gradually from the start of the aeration, and reaches about 40,000 μatm after about 4,000 s. After the start of the wind blowing, pCO_2 decreases steadily due to the transfer of CO_2 from the water side to the air side.

In Fig. 6, the time variations of pCO_2 during the flux measurement are plotted for the cases of x = 9.0 m with Ur = 4.0, 8.0 and 12.0 m/s. We should note that they are nondimensionalized by the value at the start of the measurement $pCO_{2\,start}$. A clear increase of the reduction rate of pCO_2 is observed as the speed of wind increases. This is due to the fact that the transfer rate of CO_2 increases with the wind speed. As mentioned in the previous section, the values of C_w, which are necessary for the estimation of the gas transfer velocity, were calculated by averaging the partial pressure decreasing with time.

Fig. 7 shows the relation between the gas transfer velocity k_L and the friction velocity u_{*a}. The data of experiments and field observations obtained by other researchers are also plotted in the figure. All the data in the figure are normalized to k_{L600} by using Eq. 9. The experimental data of Komori et al. (4) and Komori and Shimada (8), and the field data of McGillis et al. (9) were obtained by local flux measurements. In addition, as the results averaged over the whole interface in a wind-wave tank, the data of Broecker et al. (10) (quoted from Jähne et al. (11)) and Ocampo-Torres et al. (12) are presented. The results in this study indicate that the transfer velocity increases steadily with the friction velocity and also increases with the fetch under the condition of the

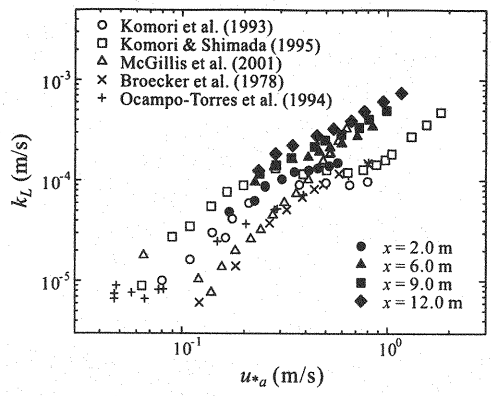

Fig. 7 Relation between k_L and u_{*a}.

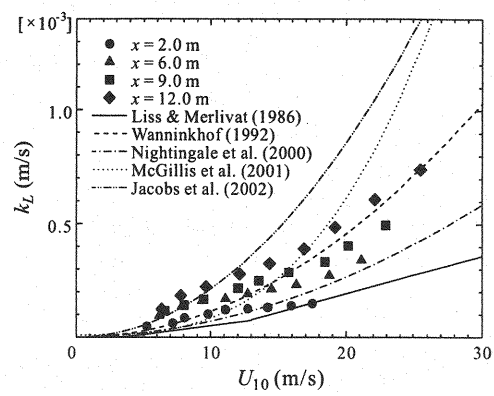

Fig. 8 Relation between k_L and U_{10}.

same friction velocity. Komori et al. suggested that the airflow separated at the wave crest reattaches in front of the leeward wave, where a high-shear region is formed and surface renewal eddies are generated. For a longer fetch, the airflow is separated more frequently, indicating that the transfer velocity may increase with the fetch if the mechanism of Komori et al. is valid for the mass transfer across the air-water interface. However, we do not have any knowledge of the fetch dependence of surface renewal eddies at present. Therefore, further investigation is necessary to verify the physical mechanism of the fetch dependence of the transfer velocity. The deviation of the present results from McGillis et al. becomes greater in the region of low friction velocities, while in the region of high friction velocities, their results are comparatively close to the present ones for longer fetch. It is also seen that the present results are relatively large compared to the fetch-averaged transfer velocity. In the case of x = 2.0 m, the increasing rate of the transfer velocity begins to decrease around u_{*a} = 0.3 m/s, and it tends to increase again in the range of high friction velocities. This behavior has been already reported by Komori et al. (4) and Komori and Shimada (8). In their experiments, the measurements were made in the region of x = 3 to 5 m. Therefore, their results correspond to the transfer velocity in the case of a short fetch. From the comparison of the present results with the results by Komori et al. and Komori and Shimada, it was deduced that the transfer velocity in the case of a short fetch shows such a behavior against the friction velocity. According to Komori et al., the reason why the transfer velocity tends to saturate in the region of intermediate friction velocities is that the energy transferred from the airflow to the water-side turbulence tends to saturate because of the energy consumption by wave growth.

In Fig. 8, the relations between the gas transfer velocity k_L and the 10-m wind speed U_{10} are shown to compare the experimental data with previous empirical expressions, in which all the data have been normalized to k_{L600}. U_{10} was calculated by extrapolating the wind speed to a height of 10 m according to the logarithmic law. The present results indicate that the increasing rate of the transfer velocity against U_{10} increases gradually with the fetch, and that the magnitude of the transfer velocity is greater than those of Liss and Merlivat (13) and Nightingale et al. (14) within the wind range in the figure. In the region of U_{10} < 10 m/s, our results except the case of x = 2.0 m agree approximately with the expression of Jacobs et al. (15), while in the region of U_{10} > 15 m/s, the results for x = 9.0 and 12.0 m approach the expression of Wanninkhof (7). The difference between the present results and the expressions of Jacobs et al. (15) and McGillis et al. (9), which are based on the eddy correlation method, is found to be large in the region of high wind speeds.

PARAMETERIZATION

At this stage of our study, we attempt to parameterize the gas transfer velocity by a dimensional analysis using the experimental data. We investigate the air-water gas transfer controlled dominantly by the resistance on the water side such as CO_2 and O_2 transfers. For growing wind waves for which the influence of swell can be

ignored, the local equilibrium is established between winds and wind-waves. In the local equilibrium state, the growth of wind waves can be determined by the fetch relations (Mitsuyasu (16)) or the 3/2-power law (Toba (17)), and dominant waves around the spectral peak frequency are regarded as gravity waves, whose the wave height and period can be determined by the friction velocity u_{*a}, the fetch x and the acceleration of gravity g. Only the gas transfer velocity under the condition of local equilibrium is chosen as the object of the parameterization. However, it should be kept in mind that capillary waves always exist on the surface of gravity wind-waves. Therefore, the gas transfer across the surface of wind waves may be also influenced by capillary waves, i.e., the surface tension, even though spectral peak waves correspond to gravity waves. Taking these arguments into account, we assume that the transfer velocity at the surface of wind waves k_L depends on the following quantities:

$$k_L = f_0(D, \nu_a, \nu_w, \rho_a, \rho_w, \gamma, g, x, u_{*a}) \tag{10}$$

where ρ_a and ρ_w are the densities of the air and water, respectively, and γ the surface tension coefficient defined as the surface tension divided by ρ_w. k_L seems to be controlled by a characteristic velocity concerning the water-side turbulence. The characteristic velocity should be affected by the momentum flux across the air-water interface, and ρ_a, ρ_w, ν_a and ν_w are considered to be physical properties concerning such a momentum transfer. Since the gas transfer is driven by the near surface turbulence and only deep-water waves are considered, the water depth is not necessary for the parameterization. According to a dimensional analysis, the transfer velocity k_L is described by the following dimensionless parameters:

$$\frac{k_L}{u_{*a}} = f_1\left(\frac{\nu_w}{D}, \frac{\nu_a}{\nu_w}, \frac{\rho_a}{\rho_w}, \frac{\gamma^3}{g\nu_a^4}, \frac{gx}{u_{*a}^2}, \frac{u_{*a}^3}{g\nu_a}\right) \tag{11}$$

Jähne et al. (6) reported that k_L depends on the Schmidt number except in the case of very low wind speed as follows:

$$\frac{k_L}{u_{*w}} \propto Sc^{-\frac{1}{2}} \tag{12}$$

This relation is widely accepted. Although Eq. 12 is expressed in terms of the friction velocity on the water side u_{*w}, this relation is also valid for the friction velocity on the air side u_{*a}, because Jähne et al. deduced u_{*w} from u_{*a} assuming the stress continuity at the water surface. The present experiments were conducted at almost the same temperature levels, thus the changes in the density and viscosity can be ignored here. Assuming that the change in the surface tension is also small, we consider the nondimensional parameters on the physical properties to be constant, i.e.,

$$\frac{\nu_a}{\nu_w} \sim \text{const.}; \quad \frac{\rho_a}{\rho_w} \sim \text{const.}; \quad \frac{\gamma^3}{g\nu_a^4} \sim \text{const.} \tag{13}$$

By considering Eqs. 12 and 13, the nondimensional transfer velocity can be expressed as follows:

$$\frac{k_L Sc^{\frac{1}{2}}}{u_{*a}} = f_2\left(\frac{gx}{u_{*a}^2}, \frac{u_{*a}^3}{g\nu_a}; \frac{\nu_a}{\nu_w}, \frac{\rho_a}{\rho_w}, \frac{\gamma^3}{g\nu_a^4}\right) \tag{14}$$

in which the parameters on the physical properties are kept constant, and two parameters gx/u_{*a}^2 and $u_{*a}^3/g\nu_a$, are varied over the experiments. gx/u_{*a}^2, which is used for the fetch relations, is a parameter related to the growth of wind waves, while $u_{*a}^3/g\nu_a$ may be interpreted as the ratio of the viscous boundary-layer thickness ν_a/u_{*a} to the wind-wave scale u_{*a}^2/g (see Csanady (18)) and it is called the Keulegan number (Keulegan (19)). Therefore, if we determine f_2 concretely, we can obtain a nondimensional empirical expression for the transfer velocity. When we examine the dependence of the nondimensional transfer velocity on gx/u_{*a}^2 or $u_{*a}^3/g\nu_a$, we have to fix the other one. In this study, we turn our attention to the surface of wind waves in the local equilibrium state, thus the experimental data that do not satisfy the fetch relations or the 3/2-power law, i.e., Ur = 4.0 to 8.0 m/s for x = 2.0 m, Ur = 4.0 to 6.0 m/s for x = 6.0 m, Ur = 4.0, 5.0 m/s for x = 9.0 m and Ur = 4.0 m/s for x = 12.0 m, should be removed from the parameterization.

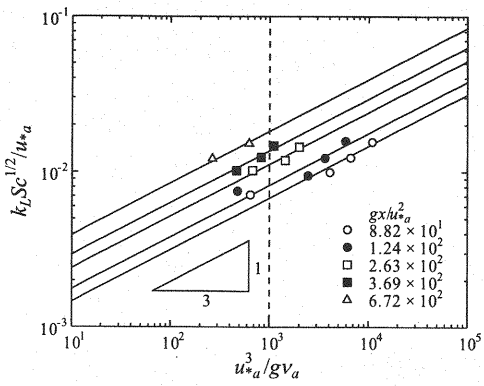

Fig. 9 Dependence of $k_L Sc^{1/2}/u_{*a}$ on $u_{*a}^3/g\nu_a$ when gx/u_{*a}^2 is remained fixed.

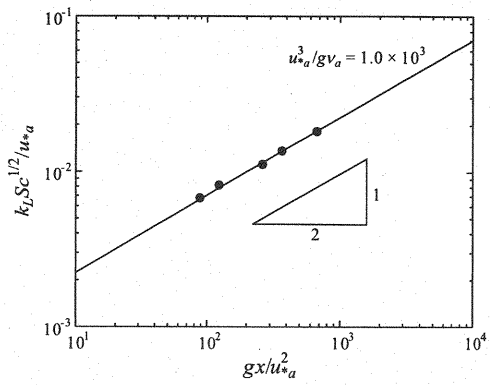

Fig. 10 Dependence of $k_L Sc^{1/2}/u_{*a}$ on gx/u_{*a}^2 when $u_{*a}^3/g\nu_a$ is remained fixed.

We found five groups whose the values of gx/u_{*a}^2 were almost the same for each group, and examined the relations between $k_L Sc^{1/2}/u_{*a}$ and $u_{*a}^3/g\nu_a$ against the same group. Fig. 9 shows the relations when the values of gx/u_{*a}^2 are remained fixed, where the solid lines indicate the fitting curves by the least square method with a 1/3-power function. It is observed from the figure that $k_L Sc^{1/2}/u_{*a}$ is proportional to $\left(u_{*a}^3/g\nu_a\right)^{1/3}$ when gx/u_{*a}^2 is kept constant. The similar relation is in approximate agreement with all the groups. This fact shows that f_2 can be expressed by the product of functions of gx/u_{*a}^2 and $u_{*a}^3/g\nu_a$.

The relation between $k_L Sc^{1/2}/u_{*a}$ and gx/u_{*a}^2 when the values of $u_{*a}^3/g\nu_a$ are set to 1.0×10^3 is plotted in Fig. 10. The data in the figure are evaluated from the intersections of the fitting curves with the dashed lines in Fig. 9. This figure shows that the data fit with a 1/2-power function, and that $k_L Sc^{1/2}/u_{*a}$ is proportional to $\left(gx/u_{*a}^2\right)^{1/2}$ when $u_{*a}^3/g\nu_a$ is fixed.

From Figs. 9 and 10, the dependence of $k_L Sc^{1/2}/u_{*a}$ on gx/u_{*a}^2 and $u_{*a}^3/g\nu_a$ is determined. Consequently, the nondimensional transfer velocity is found to be

$$\frac{k_L Sc^{\frac{1}{2}}}{u_{*a}} = A\left(\frac{gx}{u_{*a}^2}\right)^{\frac{1}{2}}\left(\frac{u_{*a}^3}{g\nu_a}\right)^{\frac{1}{3}} \tag{15}$$

where A is a constant of proportionality. In Fig. 11, the relation between $k_L Sc^{1/2} \Big/ \left[u_{*a}\left(gx/u_{*a}^2\right)^{1/2}\right]$ and $u_{*a}^3/g\nu_a$ is drawn to verify the validity of Eq. 15 for the experimental data. The fetch dependence of the transfer velocity appears to vanish and the data are normalized to a universal relation. The solid line gives an empirical expression for the transfer velocity determined by the least square method and it is written as

$$\frac{k_L Sc^{\frac{1}{2}}}{u_{*a}} = 7.17 \times 10^{-5}\left(\frac{gx}{u_{*a}^2}\right)^{\frac{1}{2}}\left(\frac{u_{*a}^3}{g\nu_a}\right)^{\frac{1}{3}} \tag{16}$$

Let us compare Eq. 16 with experimental data of other researchers to reconfirm the validity of the parameterization. Fig. 12 shows the relation of $k_L Sc^{1/2} \Big/ \left[u_{*a}\left(gx/u_{*a}^2\right)^{1/2}\right]$ with $u_{*a}^3/g\nu_a$ for the data of other researchers. The solid line indicates the empirical expression in this study (Eq. 16). Here, the experimental data of Komori et al. (4) and Komori and Shimada (8) correspond to those for the fetch of $x = 4$ m. On the other hand, in the case of the experiments performed by Broecker et al. (10) and Ocampo-Torres et al. (12), an effective fetch may be a half length of the whole interface. Thus, we assume that the fetches for Broecker et al. and Ocampo-Torres et al. are $x = 9$ and 8 m, respectively. The data of Komori et al. and Komori and Shimada are found to be proportional to 1/3-power of $u_{*a}^3/g\nu_a$, and the behavior agrees approximately with Eq. 16. The results of Broecker et al. and Ocampo-Torres et al. in the region of high wind speeds also tend to be in proportion to 1/3 power, though they take somewhat smaller values than Eq. 16. It can be deduced from these comparisons that it is possible to apply the present parameterization to the data of other researchers.

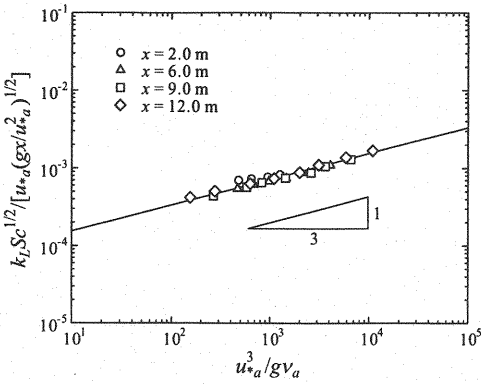

Fig. 11 Relation between $k_L Sc^{1/2}/u_{*a}$ scaled by gx/u_{*a}^2 and $u_{*a}^3/g\nu_a$.

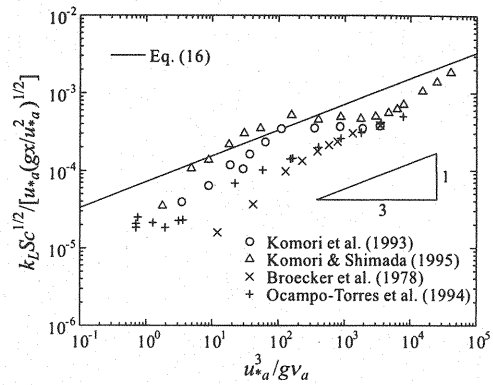

Fig. 12 Comparison of the empirical expression with other experimental data.

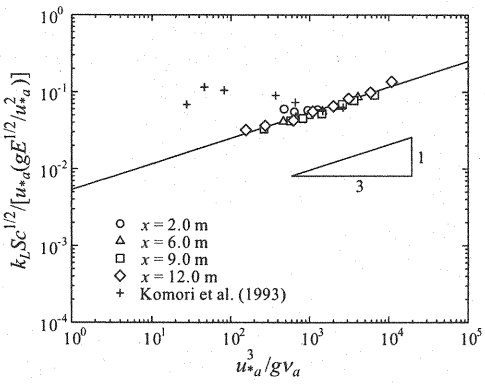

Fig. 13 Relation between $k_L Sc^{1/2}/u_{*a}$ scaled by $gE^{1/2}/u_{*a}^2$ and $u_{*a}^3/g\nu_a$.

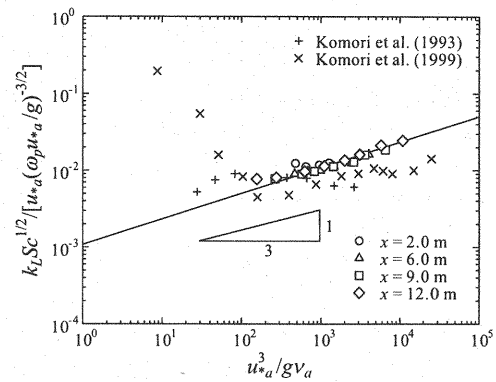

Fig. 14 Relation between $k_L Sc^{1/2}/u_{*a}$ scaled by $\omega_p u_{*a}/g$ and $u_{*a}^3/g\nu_a$.

In Eq. 16, the nondimensional transfer velocity is given by the function of gx/u_{*a}^2. It may be difficult to determine the fetch in a field, though in a laboratory experiment it can be easily evaluated. Hence, it is convenient from the view point of practicality to convert gx/u_{*a}^2 to an alternative local wind-wave parameter. Now, we can replace gx/u_{*a}^2 with the nondimensional energy $gE^{1/2}/u_{*a}^2$ or the wave-wind coefficient $\omega_p u_{*a}/g$ by using the fetch relations. Figs. 13 and 14 show the normalized relations based on $gE^{1/2}/u_{*a}^2$ and $\omega_p u_{*a}/g$, respectively. In these figures, the experimental data of Komori et al. (4), (20) are also plotted; the values of ω_p for Komori et al. (20) were calculated from the values of $R_B = u_{*a}^2/\nu_a\omega_p$ given in their paper. It should be noted here that the present results which do not satisfy the fetch relations are removed. Naturally, the nondimensional relations using $gE^{1/2}/u_{*a}^2$ or $\omega_p u_{*a}/g$ instead of gx/u_{*a}^2 can be expressed universally with a high accuracy. By estimating the fitting curves for the present results by the least square method, empirical expressions based on the local wind-wave parameters are obtained as follows:

$$\frac{k_L Sc^{\frac{1}{2}}}{u_{*a}} = 5.37 \times 10^{-3} \left(\frac{gE^{\frac{1}{2}}}{u_{*a}^2}\right)\left(\frac{u_{*a}^3}{g\nu_a}\right)^{\frac{1}{3}} \tag{17}$$

$$\frac{k_L Sc^{\frac{1}{2}}}{u_{*a}} = 1.08 \times 10^{-3} \left(\frac{\omega_p u_{*a}}{g}\right)^{-\frac{3}{2}}\left(\frac{u_{*a}^3}{g\nu_a}\right)^{\frac{1}{3}} \tag{18}$$

It appears that the results by Komori et al. (4), (20) agree approximately with Eqs. 17 and 18 in the region of high

wind speeds, while in the region of low wind speeds the difference becomes large. The reason for this may be due to the fact that their results were estimated at the fetch of $x = 4.0$ m, and that wind waves did not grow enough under the conditions of low wind speeds at which the fetch relations are invalid.

We have obtained the empirical expressions for the transfer velocity, i.e., Eqs. 16, 17 and 18. These are quite equivalent through the fetch relations. Eqs. 17 and 18 are expressed in terms of the local wind-wave parameters consisting of the friction velocity, the total energy and the spectral peak frequency of wind waves, and they are of much practical use. However, we should note that these empirical expressions cannot be applied to the surface of wind waves for which the fetch relations and the 3/2-power law are unsatisfactory, i.e., wind waves do not grow, or the influence of swell cannot be ignored.

CONCLUSIONS

We conducted laboratory experiments in a wind-wave tank in order to examine the parameterization of CO_2 transfer velocity at the surface of wind waves. In these experiments, the vertical profiles of the wind speed and the concentration of CO_2 in the air were measured at several fetches, and the local CO_2 flux was estimated by using the profile method. The concentration of dissolved CO_2 in the water was quantified by using the gas-liquid equilibrator. From these experimental results, the local transfer velocity on the water side was deduced. It was revealed that the transfer velocity increases steadily with the friction velocity, and that it also increases with the fetch under the condition of the same friction velocity. In addition, the transfer velocity in the present study became relatively larger than that averaged over the whole interface obtained by other researchers. With regard to the dependence on U_{10}, in the region of $U_{10} < 10$ m/s, the present results agreed approximately with the empirical expression of Jacobs et al. (15) except the case of $x = 2.0$ m, while in the region of $U_{10} > 15$ m/s, the results in the cases of $x = 9.0$ and 12.0 m were comparatively close to the expression of Wanninkhof (7). On the basis of the experimental results and the dimensional analysis, we parameterized the gas transfer velocity of CO_2 in consideration of the fetch dependence. Two dimensionless parameters gx/u_{*a}^2 and $u_{*a}^3/g\nu_a$, which control the mass transfer across the surface of wind waves, were derived from the dimensional analysis. The empirical expression for the transfer velocity, i.e., Eq. 16, was presented in terms of these parameters. With the fetch relations, the empirical expressions using $gE^{1/2}/u_{*a}^2$ or $\omega_p u_{*a}/g$ instead of gx/u_{*a}^2 were derived as shown in Eqs. 17 and 18, respectively. These expressions are formulated by only the local wind-wave parameters and may be of much practical use in the sense that they do not include the fetch.

The findings of this study were obtained in the fetch-limited wind-wave tank. However, since wind waves are thought to be a fluid phenomenon with the strong dynamic similarity, we think that it may be possible to apply the empirical expressions in this study to a field ocean for which the fetch relations and the 3/2-power law are satisfied. We will inspect the validity of the empirical expressions for field data by carrying out detailed observations in the future.

ACKNOWLEDGMENTS

The authors thank Profs. N. Matsunaga and T. Karasudani for helpful discussions, and the contributions made by D. Furutera, T. Ohga and D. Miyazaki to the experiments. Thanks are extended to K. Marubayashi and M. Ishibashi and H. Katayama for their useful advice and suggestion. This work has been partially supported by Grant-in-Aid for Scientific Research from Japan Society for the Promotion of Science.

REFERENCES

1. Zhao, D., Y. Toba, Y. Suzuki and S. Komori : Effect of wind waves on air-sea gas exchange: Proposal of an overall CO_2 transfer velocity formula as a function of breaking-wave parameter, *Tellus*, Vol. 55B, pp.478–487, 2003.

2. Jähne, B., T. Wais, L. Memery, G. Caulliez, L. Merlivat, K.O. Münnich and M. Coantic : He and Rn exchange experiments in the large wind-wave facility of IMST, *J. Geophys. Res.*, Vol. 90, pp.11989–11997, 1985.

3. Toba, Y. and M. Koga : A parameter describing overall conditions of wave breaking, whitecapping, sea-spray production and wind stress, *Oceanic Whitecaps*, edited by E.C. Monahan and G. Mac Niocaill, pp.37–47, D.Reidel, 1986.

4. Komori, S., R. Nagaosa and Y. Murakami : Turbulence structure and mass transfer across a sheared air-water interface in wind-driven turbulence, *J. Fluid Mech.*, Vol.249, pp.161–183, 1993.

5. Weiss, R. F. : Carbon dioxide in water and seawater: The solubility of a non-ideal gas, *Mar. Chem.*, Vol.2, pp.203–215, 1974.

6. Jähne, B., K.O. Münnich, R. Bösinger, A. Dutzi, W. Huber and P. Libner : On the parameters influencing air-water gas exchange, *J. Geophys. Res.*, Vol.92, pp.1937–1949, 1987.

7. Wanninkhof, R. : Relationship between wind speed and gas exchange over the ocean, *J. Geophys. Res.*, Vol.97, pp.7373–7382, 1992.

8. Komori, S. and T. Shimada : Gas transfer across a wind-driven air-water interface and the effects of sea water on CO_2 transfer, *Air-Water Gas Transfer*, edited by B. Jähne and E.C. Monahan, pp.553–569, AEON, 1995.

9. McGillis, W.R., J.B. Edson, J.E. Hare and C.W. Fairall : Direct covariance air-water CO_2 fluxes, *J. Geophys. Res.*, Vol.106, pp.16729–16745, 2001.

10. Broecker, H.C., J. Petermann and W. Siems : The influence of wind on CO_2-exchange in a wind-wave tunnel, including the effect of monolayers, *J. Mar. Res.*, Vol.36, pp.595–610, 1978.

11. Jähne, B., K.O. Münnich and U. Siegenthaler : Measurements of gas exchange and momentum transfer in a circular wind-water tunnel, *Tellus*, Vol.31, pp.321–329, 1979.

12. Ocampo-Torres, F., M.A. Donelan, N. Merzi and F. Jia : Laboratory measurements of mass transfer of carbon dioxide and water vapour for smooth and rough flow conditions, *Tellus*, Vol.46B, pp.16–32, 1994.

13. Liss, P.S. and L. Merlivat : Air-sea gas exchange rates: Introduction and synthesis, *The Role of Air-Sea Exchange in Geochemical Cycling*, edited by P. Baut-Ménard, pp.113–127, D. Reidel, 1986.

14. Nightingale, P.D., G. Malin, C.S. Law, A.J. Watson, P.S. Liss, M.I. Liddicoat, J. Boutin and R.C. Upstill-Goddard : In situ evaluation of air-sea gas exchange parameterizations using novel conservative and volatile tracers, *Global Biogeochem. Cycles.*, Vol.14, pp.373–387, 2000.

15. Jacobs, C., J.F. Kjeld, P. Nightingale, R. Upstill-Goddard, S. Larsen and W. Oost : Possible errors in CO_2 air-sea transfer velocity from deliberate tracer releases and eddy covariance measurements due to near-surface concentration gradients, *J. Geophys. Res.*, Vol.107, 3128, doi:10.1029/2001JC000983, 2002.

16. Mitsuyasu, H. : On the growth of the spectrum of wind-generated waves (I), *Rep. Res. Inst. Appl. Mech., Kyushu Univ.*, Vol.16, pp.459–482, 1968.

17. Toba, Y. : Local balance in the air-sea boundary processes. I. On the growth process of wind waves, *J. Oceanogr. Soc. Japan*, Vol.28, pp.109–120, 1972.

18. Csanady, G.T. : *Air-Sea Interaction: Laws and Mechanisms*, Cambridge University Press, 2001.

19. Keulegan, G.H. : Interfacial instability and mixing in stratified flows, *J. Res. Nat. Bur. Stand.*, Vol.43, pp.487–500, 1949.

20. Komori, S., T. Shimada and R. Misumi : Turbulence structure and mass transfer at a wind-driven air-water interface, *Wind-over-Wave Couplings: Perspectives and Prospects*, edited by S.G. Sajjadi, N.H. Thomas and J.C.R. Hunt, pp.273–285, Oxford University Press, 1999.

APPENDIX – NOTATION

The following symbols are used in this paper:

A	=	constant of proportionality of Eq. 15;
C_*	=	representative concentration of CO_2 estimated from the logarithmic law for CO_2;
C_a, C_w	=	concentrations of CO_2 in the air and water, respectively;
C_s	=	concentration of CO_2 on the water side at the air-water interface;
D	=	molecular diffusivity of CO_2 in the water;
E	=	total energy of the surface displacement;
F	=	CO_2 flux;
f_0, f_1, f_2	=	functions in Eqs. 10, 11 and 14, respectively;
g	=	acceleration of gravity;
H_s	=	significant wave height;
k_L	=	gas transfer velocity of CO_2 on the water side;
k_{L600}	=	gas transfer velocity for the fresh water at the standard reference temperature 20°C;
K_t	=	eddy diffusivity of CO_2;
pCO_2	=	partial pressure of dissolved CO_2 in the water;
PCO_{2s}	=	partial pressure of CO_2 on the air side at the air-water interface;
$pCO_{2\,\mathrm{start}}$	=	partial pressure of dissolved CO_2 in the water at the start of the flux measurement;
R_B	=	dimensionless parameter proposed by Toba and Koga (3), $u_{*a}^2/\nu_a\omega_p$;
S	=	solubility of CO_2 in the water;
Sc	=	Schmidt number, ν_w/D;
T	=	water temperature;
u_{*a}, u_{*w}	=	friction velocities on the air side and water side, respectively;
Ur	=	reference wind speed;
U_{10}	=	mean wind speed referred to 10 m height;
x	=	fetch;
z	=	vertical coordinate axis taken upward from the still water surface;
z_0	=	roughness length;
γ	=	surface tension coefficient;
ΔpCO_2	=	difference in partial pressure of CO_2 across the air-water interface (= $pCO_2 - PCO_{2s}$);
κ	=	von Kármán constant (= 0.4);
ν_a, ν_w	=	kinematic viscosities of the air and water, respectively;
ν_t	=	eddy viscosity;
ρ_a, ρ_w	=	densities of the air and water, respectively; and
ω_p	=	spectral peak angular frequency of wind waves.

(Received June 28, 2004; revised September 21, 2004)